Scientific Research Publishing

Journal of Geographic Information System, 2024, 16, 259-275
https://www.scirp.org/journal/jgis
ISSN Online: 2151-1969
ISSN Print: 2151-1950

Spatio-Temporal Dynamics of Land Use Units in the Kadzel Sub-Catchment Basin in Diffa, Niger

Karema Ary Madou Kaoulé[1*], Moussa Mamoudou Boubacar[1], Amadou Issoufou Abdorhimou[1], Mahamane Ali[1,2]

[1]Faculty of Agronomic Sciences, University of Diffa, Diffa, Niger
[2]Faculty of Science and Technology, Abdou Moumouni University of Niamey, Niamey, Niger
Email: *madoukaoulekaremaary@gmail.com

How to cite this paper: Kaoulé, K.A.M., Boubacar, M.M., Abdorhimou, A.I. and Ali, M. (2024) Spatio-Temporal Dynamics of Land Use Units in the Kadzel Sub-Catchment Basin in Diffa, Niger. *Journal of Geographic Information System*, **16**, 259-275.
https://doi.org/10.4236/jgis.2024.164016

Received: June 22, 2024
Accepted: July 28, 2024
Published: July 31, 2024

Copyright © 2024 by author(s) and Scientific Research Publishing Inc.
This work is licensed under the Creative Commons Attribution International License (CC BY 4.0).
http://creativecommons.org/licenses/by/4.0/

Open Access

Abstract

Environmental degradation linked to land occupation and use, such as climate change and anthropogenic activities, has led to the modification of the landscape units of the Kadzel sub-watershed. The objective of this study is to analyze the dynamics of land use units in the Kadzel area in Diffa between 1992 and 2022 and to propose a future scenario for sustainable environmental management. The approach used relies on remote sensing and geographic information systems to analyze the dynamics of land use units. Additionally, the Markov Cellular Automata (CA) model was used to predict future land use. The land cover maps were produced from a supervised classification by maximum likelihood based on the true and false color compositions of bands 4/3/2 (TM5), 3/2/1 (ETM+) and 7/5/4 (8 OLI). Ten occupation classes were discriminated. Between 1992 and 2022, there was a decrease in the areas of irrigated crops (4.91% and 2.88%), of shrubby tree steppes (14.31% and 9.48%), field-fallow complexes (22.23% and 10.52%), and degraded areas. Grassy steppes (25.76% and 13.32%). However, this reduction has been beneficial for wastelands, urban areas and bodies of water. Based on predictive modeling, it is predicted that by 2052, urban areas, fallow field complexes and bare soils will constitute the main types of housing units. The regressive trend in natural resources appears to continue into the future with current land use practices.

Keywords

Occupation Dynamics, Environmental Problems, Population Growth, Lake Chad and Kadzel Basin

1. Introduction

The dynamics of land use in arid and semi-arid regions of Africa have emerged

as a priority for decision makers and scientists alike since the widespread drought period (1970-1989) in the Sahel region [1]. Long periods of insufficient water and the gradual settlement of nomadic groups have damaged and overused fragile ecosystems, especially tree-shrub steppes [2]. On the one hand, the security crisis (refugee and displaced population settlement) has an impact on the Diffa region and causes the degradation of ecosystems in general, and woody resources in particular. However, the destruction of plant cover by refugees and the displaced deprives the soil of its natural protection, with harmful consequences for the water regime (drops in the water table) and greatly accelerates water and wind erosion [3].

Indeed, the latter is linked to insecurity, extension of cultivated areas, overgrazing, deforestation, and tree pruning [4]. We see that this weakening is manifested by the modification in the structure of the vegetation and the floristic composition [5]. The latter is detrimental to the living conditions of rural populations and the local economy [6].

Finally, in the current context of global change, spatiotemporal changes in land use, especially vegetation, have become indicators that make it possible to assess ecosystem health [7].

Therefore, this study aimed to analyze the dynamics of land use in the Kadzel area over 30 years. Additionally, it seeks to confirm the hypothesis that the study area's land use units have changed along with the landscape; natural formations have declined in favor of anthropomorphized formations, such as fields, fallows, and agglomerations; and by 2052, field-fallow complexes and agglomerations with the profile of other units dominate land use units.

2. Methodology

2.1. Study Zone

The study was carried out in the Kadzel area, located in the southeast of the Manga countryside in the Diffa region between the towns of Maïné-Soroa to the southwest and N'Guigmi to the northeast. To the south, the plain descends slightly to the valley of the Komadougou Yobé river. To the east of Kadzel are the ancient shore of Lake Chad and the desert valley to the north. The inhospitable and sparsely populated plain extends over an area of approximately 7500 km^2 (**Figure 1**). The climate is Sahelian, the annual averages of minimum and maximum temperatures are respectively 22˚C ± 28.61˚C and 39˚C ± 43˚C, and the cumulative annual precipitation is 200 to 400 mm. Relative humidity varies between 19% and 70% [8]. The dry period extends from the beginning of June to the end of September, and the wet period in the Sahel is in August (**Figure 2**). It is the rainiest month, where the average optimum rainfall reaches 135.23 ± 32.25 mm. This corresponded to a period of strong vegetation growth. Most plants grew and developed during this period, with the exception of *Faidherbia albida*. The region's vegetation consists mainly of steppes (covered with shrubs, grasses and trees) and gallery forests along watercourses. The hydrographic network of

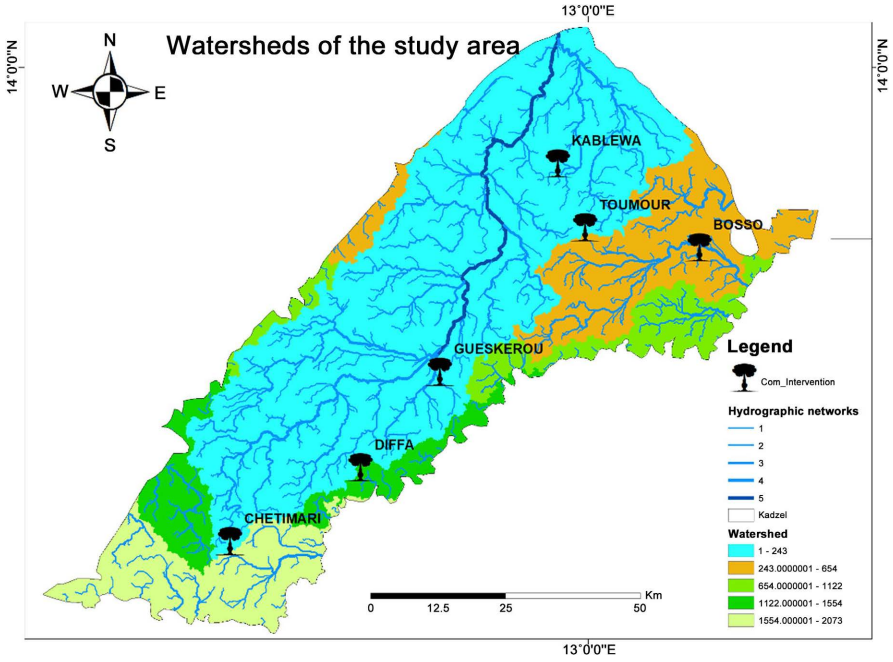

Figure 1. Location of the study area.

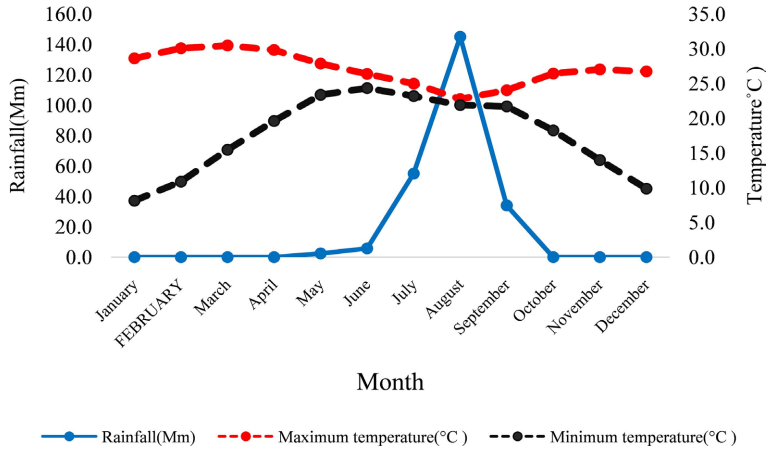

Figure 2. Ombrothermic diagram of the Kadzel zone from 1992 to 2022.

the study area is mainly composed of Komadougou Yobé, Lake Chad, and temporary pools during the wintering period in certain lowlands.

2.2. Data Collection and Analysis

Satellite images from Thematic Mapper (TM5) sensors for 1992, Landsat 7 ETM+ for 2002 and Landsat 8 OLI for 2012 and 2022. Scenes 186/050, 186/051 and 185/050 for the four different dates were downloaded from Google Earth Engine (Table 1). These data were used to produce maps of land use dynamics in the study area for the years 1992, 2002, 2012 and 2022 respectively. The choice of the dates of the images was guided by the major climatic events that occurred (periods of flooding), the evolution of agricultural practices and deforestation (the felling of trees for firewood and the manufacture of charcoal).

Table 1. Scene acquisition dates.

Contact details	Scene 1	Scene 2	Scene 3
Path	186	186	185
Row	51	50	50
Satellites			
Landsat TM5	02/09/1992	02/09/1992	05/09/1992
Landsat 7 ETM+	07/09/2002	07/09/2002	11/09/2002
Landsat 8 OLI	16/09/2012	16/09/2012	22/09/2012
	22/09/2022	22/09/2022	23/09/2022
Pixel Size	30 × 30	30 × 30	30 × 30

2.2.1. Mosaicing

The study area was covered by three (3) Landsat image scenes. These were scenes 186/050 and 186/051. Before processing, images were mosaicked. Mosaicing involves juxtaposing identical strips of scenes to form one larger strip [9]. First, the images were enhanced to standardize the hues of their spectral bands of different images [10]. Furthermore, although images from satellites differ, it is not uncommon for two adjacent images (scenes) to not have the same brightness, which causes a strong contrast to appear. To address the issue of brightness variations across images, we performed local contrast enhancement in two stages [11]. First, we homogenized the radiometric distribution for every image using radiometric stretching, also known as histogram equalization. Second, we performed a dynamic adjustment between multiple images. Radiometry of the corrected image was calibrated to match the reference images.

The study area was delimited from mosaic images, and the administrative boundaries of the municipality were extracted using the Google Earth Aegina software. The spectral characteristics of objects allow the creation of color visuals through colored composition. According to [12], its main application is to differentiate various objects in images to aid interpretation. In this treatment, the true color compositions of bands 4/3/2 of Landsat (TM5) for 1992 and the false color compositions of bands 3/2/1 of Landsat ETM+ for 2002 and 7/5/4 of Landsat 8 OLI for 2012 and 2022, respectively, were used to discriminate the different land cover units of the study area (**Figure 3**).

2.2.2. Classification

When using supervised classification, the computer algorithm specifies the numerical descriptors of the different types of land cover present in the scenery, allowing the image analyst to oversee the pixel categorization process. Thus, representative samples of known sites (training plots) were used to establish a key numerical characteristic that best described the spectral attributes of each class type. In this case, the chosen parametric algorithm is the maximum likelihood.

Each landscape unit's spectral signature could be identified as the training region that was typical of the classes' numerical attributes. To prevent the

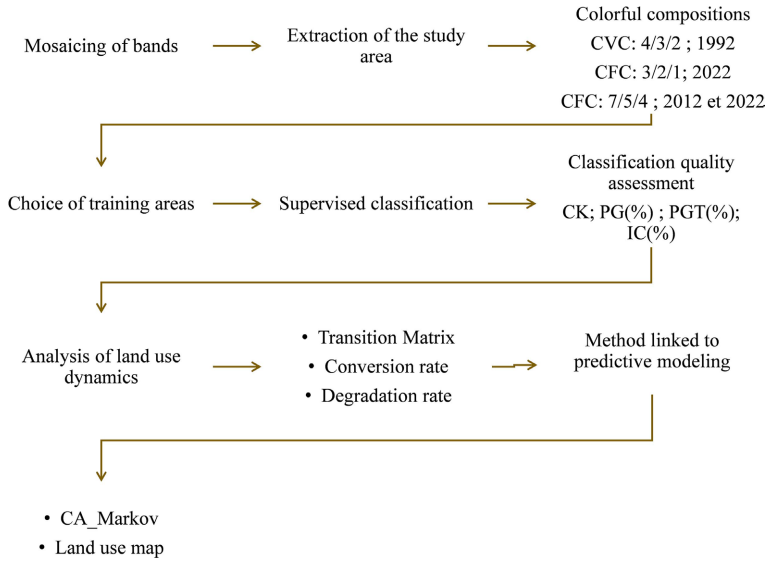

Figure 3. Summary of analysis and data processing. CFC: false color compositions; CVC: true color compositions; CK: Kappa coefficient; PG (%): Automatic Global Precision; PGT (%): Overall Field Precision; CI (%): confidence interval.

inclusion of mixed pixels (*i.e.*, pixels that could be divided into two different classes), the training regions were marked off from the transition zones [12]. The training areas were evenly distributed across the study area and were traced to the closest pixels. Each class of landscape unit was represented by these diverse training areas. As the classes became more diverse, there were more training areas [12], the dimensions of the training area must be both smaller than the object to be recognized and larger than the localization error [13], the estimate was calculated as (**Figure 3**).

$$A = P(1+2L) \tag{1}$$

where A is the surface area of the training area, P is the pixel dimension in meters, and L is the location accuracy in meters.

2.2.3. Assessment of Classification Quality

The validation of this classification using ground truth only concerned 2022 maps. Thus, to check the reliability of the provisional maps, control points were taken in each occupancy unit of the maps produced and compared with reality on the ground using GPS. This made it possible to verify their agreement and calculate the overall precision of each map in the field [14]. This index, between 0 and 1, also results from a confusion matrix based on the projection of land use units from provisional maps onto the ground. Thus, 100 points were checked in Chetimari, 123 in Diffa, 34 in Guskérou, 98 in Bosso, 58 in Tumor, and 119 in Kabléwa, resulting in a total of 474 control points in the study area.

Thus, for each classification, fairly common and widely used measures such as overall precision, Kappa coefficient, and overall field precision [15] were calculated.

In addition, overall precision and 95% confidence intervals (CI) were calculated.

$$I_c = \sqrt{a}\frac{1-a}{N} * 1.96 \quad (2)$$

CI: 95% confidence interval; a: overall precision; N = Number of observations.

$$K = \frac{a-b}{1-a} \text{ avec } a = \frac{1}{N}\sum_{i=1}^{N_c} x_{ii} \text{ et } b = \frac{1}{N^2}\sum_{i=1}^{N_c}\left(x_{+i} \cdot x_{i+}\right) \quad (3)$$

N_c: Total number of classes; N: Total number of observation points; x_{ii}: number of observation points in column i and row i corresponding to the diagonal of the matrix; x_{i+} = total number of observation points in column i (total number of observation points in the matrix); x_{+i} is the total number of observation points in row i (total at the bottom of the matrix). In total, ten land use classes were identified. These included gallery forest (forest_G), degraded shrubby tree steppe (Stp_Aa_D), shrubby tree steppe (SteppAa_D), fallow-pasture complex (Complex_J_P), degraded grassy steppe (Stp_H_D), irrigated cultivation zone (Z_C_I), agglomerations (Agglom), field-fallow complex (ComplexC_J), bare soil, and water bodies.

2.2.4. Vectorization and Cartographic Representation

Vectorization constitutes the final stage of the image processing. It consisted of converting the classified images from raster mode to vector mode (polygons) to facilitate their management in the GIS analysis software ArcGIS 10.8 [16]. The cartographic drafting consisted of producing land-use maps for 1992, 2002, 2012, and 2022 (**Figure 3**).

2.2.5. Analysis of Land Use Dynamics

1) Transition Matrix

The transition matrix makes it possible to highlight the different forms of conversion that landscape units have undergone over two years. The areas of these different classes of landscape units were calculated from the intersection of land use maps (interset) from 1992 to 2002, 2002 to 2012, and 2012 to 2022 using the ArcGIS extension. 10.8. [17] (**Figure 3**).

2) Conversion rate

According to [17], a land-use class's conversion rate reflects the level of change it experiences when changing to different classes. The evolution of land use was assessed by comparing the surface areas of land use units in different years. This rate makes it possible to quantify the changes obtained at the level of a land-use unit between the two years. It is calculated from the transition matrix using the following formula:

$$T_c = \frac{\left(S_{it} - S_{is}\right)}{S} * 100 \quad (4)$$

where T_c is the conversion rate, S_{it}: Area of landscape unit i on the initial date t, and S_{is}: Area of the same unit remaining stable on date t_1.

3) Degradation rate

The rate of degradation for each of the two periods, 1992-2002, 2002-2012, and 2012-2022, was calculated from the surface area data for the land use classes. The formula described by [18]. Was used [19]. The rate of degradation, *Td*, is expressed as a percentage (%) of the surface area per year using the following formula:

$$Td = \left[1 - \left(1 - \left(\frac{A_1 - A_2}{A_1}\right) * \frac{1}{t}\right)\right] * 100 \quad (5)$$

where Td is the degradation rate; A_1 and A_2 are the initial and final areas of the land cover units, respectively; and t is the time interval in which we want to evaluate changes in land cover.

2.2.6. Method Linked to Predictive Modeling

1) Choice of model

For the simulation of land cover, we chose the CA_Markov model for its performance, multi-scale potential, spatially explicit procedure based on raster data, and the fact that it has been successfully applied multiple times in tropical regions [20]. This model combines Markov chains, Evidential Markov chains (EMC), and cellular automata [21]. Markov chain analysis predicts future land-use patterns based on the knowledge of past and present land-use patterns. To better spatialize and comprehend the change, it is further enhanced by the use of cellular automata and a multi-criteria evaluation of a specific number of change criteria [21].

2) Development of criteria integrated into the model

For the EMC, environmental variables that are likely to affect the dynamics of land use were identified and weighted. The purpose of identifying and weighing these variables was to produce suitability maps for each land use class.

3) Identification of criteria

The number of explanatory variables to be integrated into the model is limited by their availability, their spatialization and their influence on the location and evolution of land use types. The number of factors presented and integrated is limited compared to the range of potentially explanatory environmental, socio-edaphic, political-economic, biophysical variables (soil and ecosystem degradation, silting of Lake Chad and Komadougou, erosion of biodiversity , legislation on natural resources, poverty, non-compliance with the texts in force and population density) listed by [22]. The choice of different capacities for each land use class was based on the work of [22].

4) Standardization of factors

The factors used had different minima and maxima values. To use them in EMC, they must be standardized at 256 Gy levels corresponding to the scale 0 - 255 (from least fit to most fit). This operation makes the factors comparable. The factors were standardized using fuzzy functions and weighted using the Saaty matrix, which returned the eigenvector of each factor.

2.2.7. Model Calibration and Validation

To simulate the dynamics of land use on a later date (2052), the model must first be calibrated using the known data. The 2022 image was the most recent and was the subject of the first test simulation calibrated using two previous dates (2002 and 2012). Images from 2002 and 2012 served as the basis for extrapolating the quantity of future land use. This was a linear extrapolation, because the simulation was based on two points in time to calibrate the model. Some authors define calibration as the process of estimating and modifying the parameters and constraints of a model to enhance the fit between the model's outputs and data. This stage is crucial because proper model parameterization determines the calibration of the findings that are produced [23].

For validation, the results of the 2052 land cover simulation were compared with those of the 2052 land cover map resulting from the classification. After visual comparison, a more in-depth analysis was performed by calculating the kappa indices to evaluate the quality of the prediction in terms of location. This evaluation produces Kappa agreement indices: 1) Kappa for the location of the grid-cell level (K location) and 2) K standard for determining the overall success rate [23]. Location indicates the location of the grid cells in the landscape. The standard indicates overall agreement.

2.2.8. Statistical Analyzes

Analysis of variance was performed to determine the rate of change in occupancy units per 30-year period. To do this, Shapiro-Wilk and Levene tests were performed to check the normality and homogeneity of the variance, respectively. Parametric ANOVA was performed when these conditions were met. R-studio software was used for all statistical analyses.

3. Results

3.1. Land Use Maps from 1992 to 2022

The mapped area covers an area of 5704.71 km^2. Ten land use types were mapped (**Figure 4**, **Figure 5**). These types were represented by the gallery forest (forest_G), degraded shrubby tree steppe (Stp_Aa_D), shrubby tree steppe (SteppAa_D), fallow-pasture complex (Complex_J_P), degraded grassy steppe (Stp_H_D), irrigated cultivation zone (Z_C_I), urban areas (Agglom), field-fallow complex (ComplexC_J), bare soil, and water bodies.

The discrimination of these different types of land-use units was significant, despite some confusion for all the defined classes (the pixels of certain land-use units of the fallow-pasture complex were confused with others). The results of the reliability analysis showed an overall accuracy of 86.2%, with a confidence interval of ±3.48% and a kappa index of 0.80. This reflects an almost perfect agreement in the quality of the image interpretation (**Table 2**). All land cover units had higher accuracy rates (>80%).

3.1.1. Spatio-Temporal Dynamics of Land Use Units (1992-2022)

The levels of bodies of water (2.14% to 16.90%), gallery forests (2.00% to 4.83%),

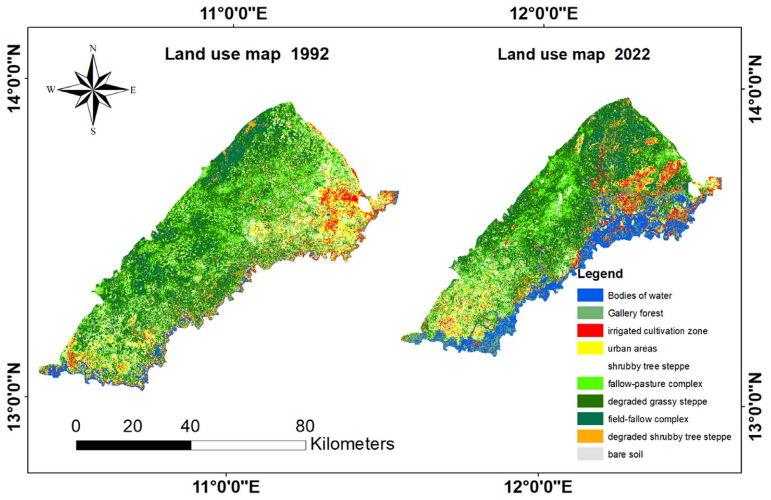

Figure 4. Land use map for 1992 and 2022.

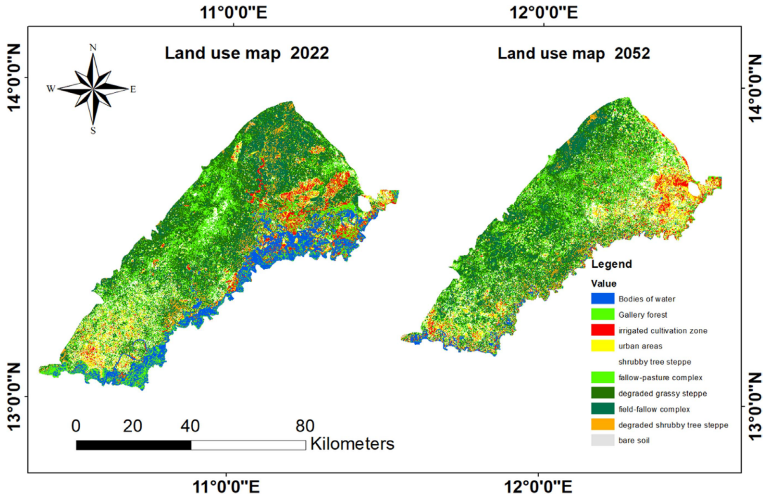

Figure 5. Land use map for the years 2022 and 2052.

Table 2. Validation index of map classifications in 1992, 2002, 2012 and 2022.

Validation indices	Kadzel area			
	Uos_1992	Uos_2002	Uos_2012	Uos_2022
Kappa coefficient	0.83	0.77	0.66	0.94
Auto Overall Accuracy (%)	89.43	82.6	73.2	87.5
Overall field accuracy (%)		86.2		
Confidence interval (CI. %)		+/−3.48%		

urban areas (9.43% to 24.79%), field-fallow complexes (15.86% to 16.28%), degraded shrubby tree steppes (3.33% to 3.76%), and bare soils (0.03% to 0.25%). In contrast, irrigated crop areas, shrubby tree steppes, fallow-pasture complexes, and degraded grassy steppes have been declining. The highest rates of conversion and degradation were observed in the tree-shrub steppes and fallow-pasture complexes (Table 3).

Table 3. Land use dynamics over the period from 1992 to 2022.

Uos	Area_1992 (%)	Area_2022 (%)	TC_1992_2022 (%)	TD_1992_2022 (%)
P_E	2.14	16.90	−8.75	0.41
Forêt_G	2.00	4.83	−4.83	−0.24
Z_C_I	4.91	2.88	−0.97	−0.02
Agglom	9.43	24.79	2.64	0.03
SteppAa_D	14.31	9.48	8.83	−7.03
Complex_J_P	22.23	10.52	5.70	−4.03
Stp_H_D	25.76	13.32	2.45	−1.01
ComplexC_J	15.86	16.28	-9.42	0.00
Stp_Aa_D	3.33	3.76	-0.44	-0.01
So_n	0.03	0.25	-0.21	-0.60
Total	100.00	100.00		

Legend: Uos: land use units, P_E: bodies of water, Forest_G: Gallery forest, Stp_Aa_D: degraded shrubby tree steppe, SteppAa_D: shrubby tree steppe, Complex_J_P: Fallow-pasture complex, Stp_H_D: degraded grassy steppe, Z_C_I: irrigated cultivation area, Agglom: urban areas, ComplexC_J: Field-fallow complex, TC: Conversion rate, TD: Degradation rate et So_n: Bare floors.

3.1.2. Quantifying Changes between 1992 and 2022

Analysis of variance for the rates of change from 1992 to 2022 showed that there was a statistically significant difference between the occupied areas at the level of all land-use units, except for gallery forests and cultivation areas. Irrigated; that is, these two units did not show statistically significant changes from 1992 to 2022 (Table 4).

3.1.3. Quantifying Changes between 1992 and 2022

The changes in land-use units between 1992 and 2022 are revealed by the transition matrix presented in Table 5. The transition matrix established between 1992 and 2022 made it possible to better characterize the changes in land use over 30 years. Indeed, 76.86% of the water body remained unchanged, with 23.86% benefiting from other units. 23.33 Of the gallery forests, 23.33% and 49.34% of the irrigated crop areas were transformed into water bodies; 6.86% of the towns were transformed into water bodies; 14.26% into gallery forests; 81.85% of shrubby tree steppe; 85.03% of fallow-pasture complex; and 87.62% of degraded grassy steppes were transformed into field-fallow complexes. 82.32 Of the field-fallow complex, 82.32% was transformed into urban areas, 91.09% of the degraded tree-shrub steppe became a field-fallow complex, and 56.90% of bare soil was transformed into a field-fallow complex (Table 5).

3.1.4. Prediction of Land Use Units for 2052

Analysis of the prediction for 2052 horizon indicated the dominance of urban areas, field-fallow complexes, and bare soils. Gallery forests (forest_G), tree-shrub

Table 4. Analysis of variance of land use units.

Uos	Area_1992 M ± σ	Area_2022 M ± σ	P_Value
P_E	122.33 ± 11.06	621.72 ± 24.93	0.0042**
Forêt_G	114.18 ± 10.68	102.67 ± 19.74	0.723
Z_C_I	279.87 ± 16.72	182.17 ± 18.3	0.821
Agglom	537.78 ± 23.19	845.21 ± 19.67	0.00543**
SteppAa_D	816.33 ± 28.571	540.79 ± 23.25	0.015**
Complex_J_P	1267.9 ± 35.6	942.59 ± 30.7	0.0023**
Stp_H_D	1469.66 ± 38.33	1330.08 ± 36.47	0.0123**
ComplexC_J	904.76 ± 30.07	928.59 ± 30.47	0.003**
Stp_Aa_D	189.84 ± 13.778	214.73 ± 14.65	0.00044**
So_n	1.99 ± 1.41	14.07 ± 3.75	0.001**

Legend: Uos: land use units, P_E: bodies of water, Forest_G: Gallery forest, Stp_Aa_D: degraded shrubby tree steppe, SteppAa_D: shrubby tree steppe, Complex_J_P: Fallow-pasture complex, Stp_H_D: degraded grassy steppe, Z_C_I: irrigated cultivation area, Agglom: urban areas, ComplexC_J: Field-fallow complex, So_n: Bare floors, M: mean et σ: Standard deviation.

Table 5. Transition matrix.

1992 / 2022	P_E	Forêt_G	Z_C_I	Agglom	SteppAa_D	Complex_J_P	Stp_H_D	ComplexC_J	Stp_Aa_D	So_n	Total
P_E	76.86	22.86	0.07	0.01	0.00	0.00	0.00	0.00	0.18	0.00	100.00
Forêt_G	23.33	56.06	20.13	0.19	0.07	0.02	0.10	0.00	0.10	0.00	100.00
Z_C_I	49.34	18.97	24.62	2.17	0.45	0.57	3.23	0.15	0.50	04.00	100.00
Agglom	6.86	14.26	0.40	70.21	0.62	1.38	4.10	2.08	0.49	0.00	100.00
SteppAa_D	2.61	4.03	0.27	1.03	0.49	2.62	6.70	81.85	0.39	0.00	100.00
Complex_J_P	1.59	1.95	0.17	0.62	0.46	2.43	7.17	85.03	0.58	0.00	100.00
Stp_H_D	1.54	1.45	0.18	0.47	0.48	1.90	5.74	87.62	0.62	0.00	100.00
ComplexC_J	1.53	1.19	0.17	82.32	0.48	2.35	10.35	0.47	1.14	0.00	100.00
Stp_Aa_D	1.22	1.07	0.17	0.30	0.48	1.28	3.35	91.09	1.02	0.02	100.00
So_n	0.00	0.02	0.14	7.10	0.85	1.57	4.75	56.90	4.02	24.64	100.00

Legend: P_E: bodies of water, Forest_G: Gallery forest, Stp_Aa_D: degraded shrubby tree steppe, SteppAa_D: shrubby tree steppe, Complex_J_P: Fallow-pasture complex, Stp_H_D: degraded grassy steppe, Z_C_I: irrigated cultivation area, Agglom: urban areas, ComplexC_J: Field-fallow complex, So_n: Bare floors.

steppes (SteppAa_D), fallow-pasture complexes (Complex_J_P), degraded grassy steppes (Stp_H_D), irrigated cultivation areas (Z_C_I), and waterbodies regressed over time. The highest rates of conversion and degradation were observed at the level of the shrubby tree steppes, gallery forest (forest_G) of the fallow-pasture complex (Complex_J_P), degraded grassy steppe (Stp_H_D), and irrigated cultivation zone (Z_C_I) (Table 6).

Table 6. Prediction of the dynamics of land use units.

Uos	Area _2022 (%)	Area _2052 (%)	TC_2022_2052 (%)	TD_2022_2052 (%)
P_E	16.9	7.15	−9.75	−2.55
Forêt_G	4.83	4.79	−2.04	−0.13
Z_C_I	2.88	1.53	2.65	0.09
Agglom	24.79	30.63	3.84	0.11
SteppAa_D	9.48	6.24	5.76	0.11
Complex_J_P	10.52	5.97	0.45	0.01
Stp_H_D	13.32	8.43	−9.89	−0.22
ComplexC_J	16.28	23.18	1.90	0.03
Stp_Aa_D	3.76	7.32	3.55	0.15
So_n	0.25	3.77	3.52	0.28
Total	**100.00**	**100.00**		

Legend: Uos: land use units, P_E: bodies of water, Forest_G: Gallery forest, Stp_Aa_D: degraded shrubby tree steppe, SteppAa_D: shrubby tree steppe, Complex_J_P: Fallow-pasture complex, Stp_H_D: degraded grassy steppe, Z_C_I: irrigated cultivation area, Agglom: urban areas, ComplexC_J: Field-fallow complex,TC: Conversion rate, TD: Degradation rate et So_n: Bare floors.

1) Quantifying changes between 2022 and 2052

A comparative analysis of the rate of change in land-use units in horizon 2052 showed a statistically significant difference between the areas at the level of all land-use units: water bodies, urban areas, tree-shrub steppe, fallow-pasture complex, field-fallow complex, degraded tree-shrub steppe, degraded grassy steppe, gallery forest, irrigated crop areas, and bare soils. A significant difference between these units indicates that they will be followed by changes in the next period until 2052 (Table 7).

2) Quantifying future changes

The transition matrix established between 2022 and 2052 made it possible to better characterize land use changes over the next 30-year period. Indeed, 46.12% of the water body remained unchanged compared to 53.88% for the benefit of the other units. A total of 46.12% of gallery forests will be transformed into irrigated crop zones, 56.36% of irrigated crop zones will be transformed into towns, 40.93% of shrubby tree steppe, 41.51% of fallow-pasture complex, and 42.22% of degraded grassy steppe will be transformed into field-fallow complexes. 82.92 Of the field-fallow complex, 82.92% was transformed into urban areas, 74.87% of the degraded tree-shrub steppe became a field-fallow complex, and 31.19% of bare soil was transformed into a field-fallow complex (Table 8).

4. Discussion

4.1. Dynamics of Land Use Units

The mapped area covers an area of 5704.71 km^2. Thus, ten land use units were

Table 7. Analysis of variance of land use units.

Uos	Area_2022 M ± σ	Area_2052 M ± σ	P_Value
P_E	65.34 ± 8.08	44.72 ± 24.93	0.0035**
Forêt_G	273.23 ± 16.52	389.67 ± 19.74	0.0011**
Z_C_I	486.43 ± 22.05	335.17 ± 18.3	0.002**
Agglom	606.55 ± 24.62	387.21 ± 19.67	0.001**
SteppAa_D	869.28 ± 29.48	540.79 ± 23.25	0.014**
Complex_J_P	968.18 ± 31.11	942.59 ± 30.7	0.0313**
Stp_H_D	766.05 ± 27.67	1330.08 ± 36.47	0.0004**
ComplexC_J	1037.13 ± 32.2	928.59 ± 30.47	0.007**
Stp_Aa_D	417.3 ± 20.42	214.73 ± 14.65	0.0013**
So_n	215.07 ± 14.66	14.07 ± 3.75	0.0012**

Legend: Uos: land use units, P_E: bodies of water, Forest_G: Gallery forest, Stp_Aa_D: degraded shrubby tree steppe, SteppAa_D: shrubby tree steppe, Complex_J_P: Fallow-pasture complex, Stp_H_D: degraded grassy steppe, Z_C_I: irrigated cultivation area, Agglom: urban areas, ComplexC_J: Field-fallow complex, So_n: Bare floors, M: mean et σ: Standard deviation.

Table 8. Transition matrix.

2022 / 2052	P_E	Forêt_G	Z_C_I	Agglom	SteppAa_D	Complex_J_P	Stp_H_D	ComplexC_J	Stp_Aa_D	So_n	Total
P_E	46.12	48.08	5.46	0.34	0.00	0.00	0.00	0.00	0.00	0.00	100.00
Forêt_G	3.81	61.82	34.18	0.18	0.02	0.00	0.00	0.00	0.00	0.00	100.00
Z_C_I	9.80	8.36	18.10	56.36	4.84	1.63	0.30	0.03	0.04	0.53	100.00
Agglom	0.91	3.68	5.30	87.42	0.92	0.41	0.19	1.09	0.03	0.04	100.00
SteppAa_D	0.12	2.03	2.41	5.53	15.33	0.79	28.12	40.93	4.67	0.07	100.00
Complex_J_P	0.01	0.15	0.65	1.39	14.05	40.57	0.99	41.51	0.65	0.02	100.00
Stp_H_D	0.01	0.10	0.45	1.64	8.06	45.41	0.43	42.22	1.64	0.03	100.00
ComplexC_J	0.00	0.00	0.23	82.92	0.96	0.56	0.30	14.11	0.46	0.45	100.00
Stp_Aa_D	0.00	0.00	0.04	1.19	9.07	0.66	0.22	74.87	13.76	0.19	100.00
So_n	0.00	0.01	0.00	0.02	0.13	5.16	28.70	31.19	28.09	6.70	100.00

Legend: P_E: bodies of water, Forest_G: Gallery forest, Stp_Aa_D: degraded shrubby tree steppe, SteppAa_D: shrubby tree steppe, Complex_J_P: Fallow-pasture complex, Stp_H_D: degraded grassy steppe, Z_C_I: irrigated cultivation area, Agglom: urban areas, ComplexC_J: Field-fallow complex, So_n: Bare floors.

defined with significant statistical precision because the Kappa index was 0.80. It can be concluded that the results of this analysis were statistically acceptable. An analysis of the dynamics of land use in the Kadzel zone shows the different forms of change that have occurred over time. Thus, the results reveal, from 1992 to 2022, a regression in the irrigated cultivation area, shrubby tree steppes, fallow-pasture complexes, and degraded grassy steppe in favor of camp-fallow

complexes, agglomerations, urban areas and water bodies. These results are consistent with those of [24] and [25] who showed continuous regression of vegetation in favor of fallow fields, bare soils, and urban areas based on a diachronic study. The creation of new fields is detrimental to the forest ecosystems [26]. In addition, the increase in agricultural land to feed an ever-increasing population justifies the reduction in the duration of fallows and the annual increase in anthropized spaces [27]. Plant formation is influenced by climate change and human activities [28]. The former are considered inevitable on a scale of a century [29], and their effects on species extinction are generally limited [30]. However, the impact of human activities is likely to cause changes in plant succession and environmental degradation of the environment [31].

The highest rates of degradation were found in the tree-shrub steppe and fallow-pasture complexes. This justifies the extension of the cultivated areas to the detriment of plant growth. This expansion of agricultural land leads to the deforestation of natural plant formations by producers in search of fertile land, probably due to the drop in crop yields but also due to population growth whose vital needs must be met to improve incomes [31]. This also corresponds to the periods of space occupation by refugees fleeing the abuse of Boko Haram in the beds of Lake Chad. We noted evolutionary trends (gains to the detriment of another type of land occupation) and regressive trends (loss of surface area to the benefit of another type of land use). Apart from agricultural activities, the felling of trees for firewood and the production of charcoal as a source of energy also constitute direct actions to destroy natural plant formations. Furthermore, the cutting of woody trees activates wind and water erosion, resulting in drainage of the arable part of the cultivated land. This situation is also one of the causes of the decline in fertility, which negatively affects crop yields and justifies the expansion of registered cultivated lands. This transformation was the result of human actions, such as deforestation and overgrazing, following a rapid increase in the population in the area, which recorded a massive flow of displaced people and refugees. With the Boko Haram crisis, the population increased from 40,923 in 2013 to 123,995 in 2017. In addition, the settlement of displaced people has contributed to the expansion of host villages. This has resulted in an increase in residential areas [31].

4.2. Prediction of Land Use Units

The prediction for 2052 indicated the dominance of urban areas, field-fallow complexes, and bare soil. The highest rates of conversion and degradation were observed at the level of the shrubby tree steppes, gallery forest (forest_G) of the fallow-pasture complex (Complex_J_P), degraded grassy steppe (Stp_H_D), and irrigated cultivation area (Z_C_I). By others found in the same area, a progressive dynamic in terms of an increase was observed in agglomerations, field-fallow complexes, and bare soils [31]. The simulation of land use contributes to the understanding of the functioning of landscaped spaces. According to [32], the importance of predictive modeling is not to precisely determine the future of a

territory but to lead decision-makers to be proactive in anticipating the instantaneous degradation of natural resources.

5. Conclusions

At the end of this study, we note that remote sensing processing and the geographic information system made it possible to analyze the dynamics of land use between the years of 1992 and 2022 and to predict land use in 2052. Study shows that the ecological balance of the Kadzel area has been greatly disrupted by the increase in population combined with anthropogenic activities. The cartographic results made it possible to highlight the different forms of conversion that the vegetation underwent in the transitional matrix. Thus, we note the regression of plant formation with an amplitude of 20.44% for the 30 years from 1992 to 2022. Plant formations have gradually given way, in part, to anthropized formations. Demography, agriculture and overgrazing are the main causes of deforestation.

Furthermore, the projection for 2052 confirms the strong anthropization of current practices of exploitation of natural resources. It is therefore important to improve agricultural production systems and breeding methods according to population growth for harmonious and sustainable development.

Conflicts of Interest

The authors declare no conflicts of interest regarding the publication of this paper.

References

[1] Sylla, D., BA, T., Dalanda Diallo, M., Mbaye, T., Diallo, A., Luc Peiry, J., *et al.* (2019) Dynamique de l'occupation du sol de la commune de Téssékéré de 1984 à 2015 (Ferlo Nord, Sénégal). *Journal of Animal & Plant Sciences*, **40**, 6674-6689. https://doi.org/10.35759/janmplsci.v40-3.2

[2] Millogo, D., Nikiema, A., Koulibaly, B. and Zombre, N.P. (2018) Analyse de l'évolution de l'occupation des terres à partir de photographies aériennes de la localité de Loaga dans la province du Bam, Burkina Faso. *International Journal of Biological and Chemical Sciences*, **11**, 2133-2143. https://doi.org/10.4314/ijbcs.v11i5.16

[3] Rabiou, H., Bationo, B. A., Adjonou, K., Kokutse, A. D., Mahamane, A. and Kokou, K. (2017) Perception paysanne et importance socioculturelle et ethnobotanique de Pterocarpus erinaceus au Burkina Faso et au Niger. *Afrique Science*, **13**, 43-60.

[4] Sylla, D., Ba, T. and Guisse, A. (2019) Cartographie des changements de la couverture végétale dans les aires protégées du Ferlo (Nord Sénégal): Cas de la réserve de biosphère. *Physio-Géo*, **13**, 115-132. https://doi.org/10.4000/physio-geo.8178

[5] Taibou, B., Akpo, L.E. and Diouf, A.A. (2017) Dynamiquespatio-temporelle des écosystèmes du bassin versant du Ferlo (Nord-Sénégal). *Journal of Animal &Plant Sciences*, **33**, 5255-5273.

[6] Aimée, D., Sambou, H., Diop, C., Ntiranyibagira, E., Dacosta, H. and Sambou, B. (2018) Dynamique d'occupation du sol des zones humides urbanisées de Dakar (Sénégal) de 1942 à 2014. *VertigO*, **18**, 48 p. https://doi.org/10.4000/vertigo.20120

[7] Arouna, O., Etene, C.G. and Issiako, D. (2016) Dynamique de l'occupation des

terres et état de la flore et de la végétation dans le bassin supérieur de l'Alibori au Benin. *Journal of Applied Biosciences*, **108**, 10543-10552. https://doi.org/10.4314/jab.v108i1.7

[8] Oumarou, H., Caremel, J.F. and Kiari Fougou, H. (2017) En Gudunhijira: Fuites, accueils, solidarités et reconfigurations économiquesencontexted'insécurités et d'aidehumanitaire dans la région de Diffa. LASDEL.

[9] Avakoudjo, J., Mama, A., Toko, I., Kindomihou, V. and Sinsin, B. (2015) Dynamique de l'occupation du sol dans le Parc National du W et sa périphérie au nord-ouest du Bénin. *International Journal of Biological and Chemical Sciences*, **8**, 2608-2625. https://doi.org/10.4314/ijbcs.v8i6.22

[10] Goussot, E., BrouYao, T. and Laouina, A. (2014) Dynamique de l'occupation du sol et statitistiquesagricoles sur le bassin versant du Bouregreg au Maroc. *European Journal of Scientific Research*, **126**, 191-205.

[11] Konan-Waidhet, A.B., Kouassi, K.H. and Kanga, K.E. (2022) Land Use Dynamics in the Department of Séguéla, Northwestern Côte d'Ivoire. *Advances in Remote Sensing*, **11**, 63-79. https://doi.org/10.4236/ars.2022.113005

[12] Seidou, A.A., Agbayigbo, A.A., Traore, I.A. and Houinato, M. (2017) Spatio-Temporal Dynamics of Natural Rangelands Exploited by Transhumance Cattle Herds in the Classified Forest of Upper Alibori, Northern Benin. *American Scientific Research Journal for Engineering, Technology, and Sciences*, **33**, 111-123.

[13] Brun, L.E., Gaudence, D.J., Gibigaye, M. and Tente, B. (2018) Dynamique De L'occupation Du Sol Dans Les Zones Humides De La Commune D'allada Au Sud-Benin (Sites Ramsar 1017 Et 1018). *European Scientific Journal*, **14**, 59-77. https://doi.org/10.19044/esj.2018.v14n12p59

[14] Biga, I., Amani, A., Soumana, I., Bachir, M. and Mahamane, A. (2020) Dynamique spatio-temporelle de l'occupation des sols des communes de Torodi, Gothèye et Tagazar de la région de Tillabéry au Niger. *International Journal of Biological and Chemical Sciences*, **14**, 949-965. https://doi.org/10.4314/ijbcs.v14i3.24

[15] Hanania, S., Honvou, S., Aboh, A.B., Tèka, O., Sèwadé, C., Gandonou, C. and Sin-sin, B. (2022) Modélisation de la dynamique de l'occupation du sol des parcours des transhumants dans la Basse et Moyenne Vallée de l 'Ouémé (Bénin). *Sciences and Technologies for Sustainable Agriculture*, 2, 18-29.

[16] Kamagaté, A., Koffi, B.Y. and Kouassi, M.A. (2019) Études prospectives appliquées à la dynamique de l'occupation et d'usage du sol et des ressources en eau: État de l'art. *International Journal of Innovation and Applied Studies*, **25**, 1408-1418.

[17] Arouna, O., Imorou, I.T., Gibigaye, M., Alle, P. and Tente, B. (2017) Comparative Analysis of the State of Conservation of Gazetted Forests, Community Forests and Sacred Forests (West Africa). *International Journal of Innovation and Applied Studies*, **19**, 123.

[18] Kpedenou, K.D., Boukpessi, T. and Tchamie, T.T.K. (2016) Quantification des changements de l'occupation du sol dans la préfecture de Yoto (sud-est Togo) à l'aide de l'imageriesatellitaire Landsat. *Sciences de l'Environnement*, **13**, 137-156.

[19] Biaou, S., Houeto, F., Gouwakinnou, G., Biaou, S.S.H., Awessou, B., Tovihessi, S. and Tete, R. (2019) Dynamiquespatio-temporelle de l'occupation du sol de la forêtclassée de Ouénou-Bénou au Nord Bénin. *Conférence OSFACO: Des images satellites pour la gestion durable des territoires en Afrique*, 21 p.

[20] Akadje, L.M.C., Kangah, A., Boussougouboussougou, G., Hauhouot, A.C. and Brou, Y. (2017) Modélisations prospectives de l'occupation du sol d'une zone à forte pression anthropique: Cas du site Ramsar de Grand-Bassam, (Sud-Est de la Côte d'Ivoire).

Cahiers du CBRST, **11**, 11-33.

[21] Kouassi, K.H., Konan-Waidhet, A.B., Yao, A.B., Koffi, B. and Kadjo, E.D. (2020) Simulation of the Dynamics of Land Cover and Land Use in the Lobo River Watershed Upstream of Nibéhibé (center-West of Côte d'Ivoire). *Journal of Geographic Information System*, **12**, 519-530. https://doi.org/10.4236/jgis.2020.125030

[22] Gasmi, A., Masse, A., Ducrot, D. and Zouari, H. (2017) Télédétection et photogrammétrie pour l'étude de la dynamique de l'occupation du sol dans le bassin versant de l'oued Chiba (Cap-Bon, Tunisie). *Revue Française de Photogrammétrie et de Télédétection*, No. 215, 43-51. https://doi.org/10.52638/rfpt.2017.344

[23] Mama, A., Sinsin, B., De Cannière, C. and Bogaert, J. (2013) Anthropisation et dy-namique des paysagesen zone soudanienne au nord du Bénin. *Tropicultura*, **31**, 78-88.

[24] Diallo, H., Bamba, I., Barima, Y. S. S., Visser, M., Ballo, A., Mama, A., Bogaert, J., *et al.* (2011) Effetscombinés du climat et des pressions anthropiques sur la dynami-queévolutive de la végétationd'une zone protégée du Mali (Réserve de Fina, Boucle du Baoulé). *Science et changementsplanétaires/Sécheresse*, **22**, 97-107.

[25] Sikuzani, Y.U., Boisson, S., Kaleba, S.C., Khonde, C.N., Malaisse, F., Halleux, J., *et al.* (2019) Dynamique de l'occupation du sol autour des sites miniers le long du gradient urbain-rural de la ville de Lubumbashi, RD Congo. *Biotechnologie, Agronomie, Société et Environnement*, **24**, 14-27. https://doi.org/10.25518/1780-4507.18306

[26] Agbanou, B.T. (2018) Dynamique de l'occupation du sol dans le secteur Natitin-gou-Boukombé (nord-ouestbénin): De l'analysediachronique à unemodélisation prospective. Master's Thesis, Université Toulouse le Mirail-Toulouse II.

[27] Bidossessi, T.A., Paegelow, M. and Tente, B. (2018) Evaluation de l'occupation du sol dans la commune de Ouake (Nord-Ouest Benin) à partir de la télédétection. In: Orekan, V.O.A., Mertens, B., Ahononga, F.C. and Brice, T., Eds., *Images satellitaires pour un meilleuraménagement des territoires et une gestion durable de la biodiversité*, 75-90.

[28] Avakoudjo, J., Kouelo, A.F., Kindomihou, V., Ambouta, K. and Sinsin, B. (2015) Effet de l'érosionhydrique sur les caractéristiquesphysicochimiques du sol des zones d'érosion (dongas) dans la Commune de Karimama au Bénin. *Agronomie Africaine*, **27**, 127-143.

[29] Tankoano, B., Sanon, Z., Hien, M., Dibi, N.H., Yameogo, J.T. and Somda, I. (2016) Pression anthropique et dynamiquevégétale dans la Forêt Classée de Tiogo au Burkina Faso: Apport de la Télédétection. *Tropicultura*, **34**,193-207.

[30] Dembélé, M., Bamani, S., Dembélé, R., Traoré, M.O., Goita, S., Traoré, M.N., *et al.* (2012) Implementing Preventive Chemotherapy through an Integrated National Neglected Tropical Disease Control Program in Mali. *PLOS Neglected Tropical Diseases*, **6**, e1574. https://doi.org/10.1371/journal.pntd.0001574

[31] Arouna, O., Imorou, I.T., Gibigaye, M., Alle, P. and Tente, B. (2017) Analyse com-parative de l'état de conservation des forêtsclassées, des forêtscommunautaires et des forêtssacrées au Sud-Bénin (Afrique de l'Ouest) [Comparative Analysis of the State of Conservation of Gazetted Forests, Community Forests, and Sacred Forests (West Africa)]. *International Journal of Innovation and Applied Studies*, **19**, 123-139.

[32] Habou, R., Mansour, M., Issiaka, I. and Ali, M. (2019) Impact de L'installation des Camps des Refugiés, Retournés et Déplacés sur L'exploitation des Ressources Ligneuses dans la Région de Diffa. *European Scientific Journal*, **15**, 118-140. https://doi.org/10.19044/esj.2019.v15n36p118